Experimental evidence for the functional relevance of anion-π interactions

Ryan E. Dawson, Andreas Hennig, Dominik P. Weimann, Daniel Emery, Velayutham Ravikumar, Javier Montenegro, Toshihide Takeuchi, Sandro Gabutti, Marcel Mayor, Jiri Mareda, Christoph A. Schalley, and Stefan Matile

Nature Chemistry **2010**, *2*, 533–538.

1. Introduction

1-1. Anion-π interactions vs. Cation-π interactions

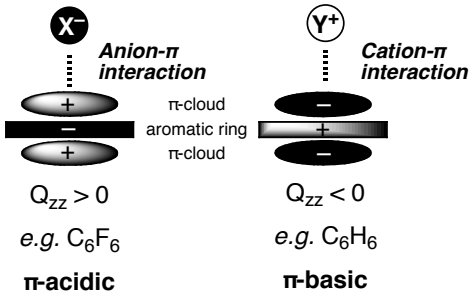

Figure 1. Schematic side view of π-acidic and π-basic aromatic rings.

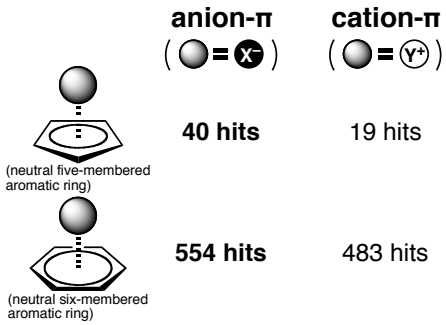

Figure 2. The results of an CSD (Cambridge Structural Database) survey.

• Anion-π interactions are defined as nonbonding interactions between an electron-deficient or π-acidic aromatic system with positive quadrupole moments Q_{zz} and an anion (Figure 1).[1]

• Contrary to general belief, anion-π interactions are more frequent than cation-π interactions (Figure 2).[2]

• Anion-π interactions was used for anion transport in the transmembrane and excellent activity and anion selectivity were found, however, it was not possible to prove experimentally that anion-π interaction really exist.[3,4]

➢ In this work, a systematic study that combines both theory and experiment was performed to provide the direct evidence for the existence of anion-π interactions.

2. Results & Discussions

2.1 Design

• NDIs (naphtalenediimides) have the largest positive Q_{zz} and distinct facial π-acidity (Table 1).

Table 1.

compound	Q_{zz} (B)
NDI	+ 20
dicyano NDI	+ 39
tetracyano NDI	+ 56
hexafluorobenzene	+ 9.5
trinitrotoluene	+ 20

• Active-site decrowding and π-acidity are systematically maximized by *o*-methyl removal in **4** and **6** and addition of cyano acceptors in the core of **5** and **6**.

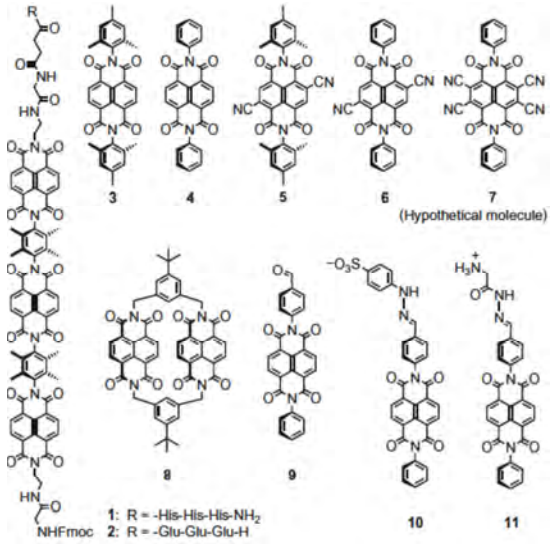

Figure 3. Structure of NDIs.

2.2 Computational study

• Electrostatic potential surfaces imply that anion binding is expected to occur at the pyridinedion heterocycles, which is the highest electron deficient region (Figure 4).

• Distance between the NDI plane and anion (R_e) decreased with increasing the π-acidity and decreasing the steric hindrances (Table 2).

• $Cl^- > Br^- > NO_3^-$ selectivity was expected from the interaction energy (E_{int}) (Table 2).

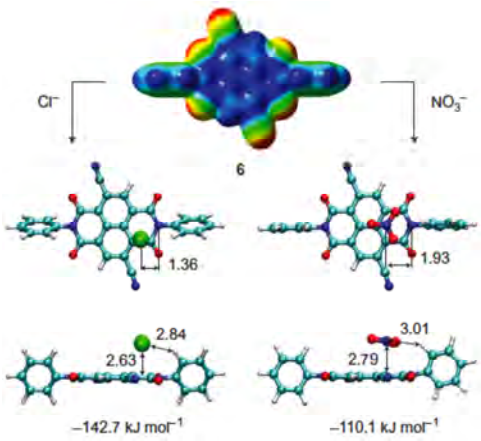

Figure 4. Molecular modeling of anion-π interactions.

Table 2. Summary of anion binding data for melecular modeling.[a, b]

NDI	R_e (Å)[a]		E_{int} (kJ mol^{-1})[b]		
	Cl^-	NO_3^-	Cl^-	Br^-	NO_3^-
3	2.86	2.97	- 83.3	- 72.0	- 69.9
4	2.85	2.87	- 92.1	- 79.9	- 69.5
5	2.70	2.86	- 136.4	- 123.1	- 110.9
6	2.63	2.79	- 142.7	- 129.8	- 110.1
7	2.50	2.74	- 188.8	- 173.7	- 143.6
8	3.02	2.93	- 121.0	- 104.6	- 95.4

[a]Equilibrium distance between chloride (nitrate) and NDI plane in monomeric complexes; [b]Interaction energy in monomeric NDI anion complexs computed with the PBE1PBE/6-311 ++G** //PBE1PBE/6-311G** method.

2.3 Direct evidence for anion-π interaction

2.3.1 NMR spectroscopy

• It was not meaningful because binding was too weak and NMR shifts were too small.

2.3.2 ESI-FTICR-MS-MS

• ESI-FTICR-MS-MS (electrospray ionization Fourier-transform ion cyclotron resonance tandem mass spectrometry) experiments appeared ideal to deliver the desired direct experimental evidence for anion-π interactions.

➢ Quite fragile NDI-anion complexes of **3–6** were observed for Cl^-, Br^- and NO_3^-.

• For example, an equimolar mixture of NDIs **3** and **4** was electrosprayed together with one equivalent of NEt_4Cl, and corresponding heterodimer **3** + **4** + Cl^- was isolated (Figure 5a)

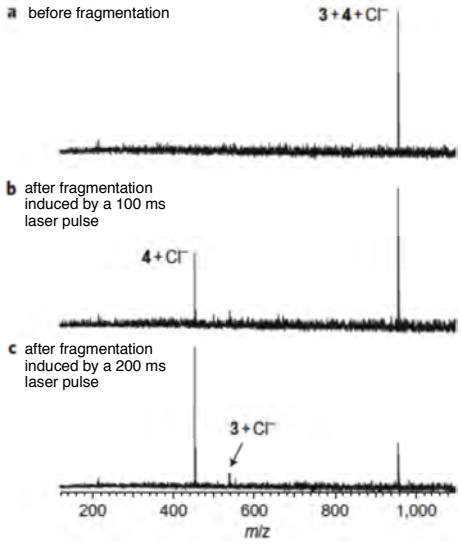

Figure 5. Laser-induced ESI-MS-MS fragmentation of heterodimer complexes.

• Fragmentation of heterodimer was induced by irradiation with IR laser.

➢ After 100 ms irradiation, Cl^- stared to appear together with monomeric NDI **4** alone (Figure 5b).

➢ After 200 ms irradiation, the peak for **3** + **4** + Cl^- nearly disappeared and a new peak for **3** + Cl^- appeared (Figure 5c)

➢ These observations demonstrated that NDI **4** binds Cl^- better than NDI **3**.

• Found selectivity sequence was **6** > **5** > **4** > **3**, suggesting increasing anion affinity with increasing π-acidity and decrowding of the anion-π binding site.

2.4 Anion transport activity

2.4.1 Vesicle-based method for measuring anion transport

• The transport activity of NDIs **2**-**11** was determined in large unilamellar vesicles (LUVs) composed of egg yolk phosphatidylcholine (EYPC) containing different fluorescent probes.

• NDIs are thought to self-assemble into transmembrane dimers of single-leaflet bundles (**c**) that are stabilized by hydrophilic head (**b**, **c**) and vertical (**b**) or horizontal (**d**) crosslinking (Figure 6).

• Anion transport occurs along the NDI surface (Figure 7).[4]

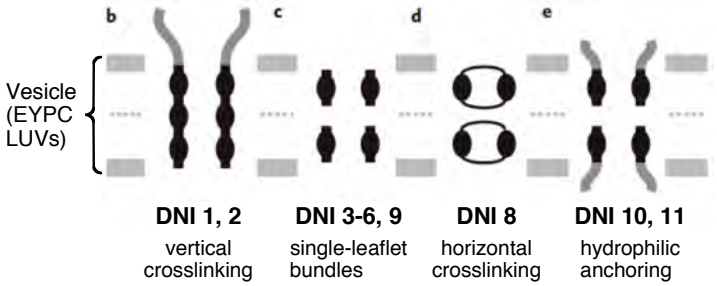

Figure 6. Hypothesized active suprastructures of anion-π transporters.

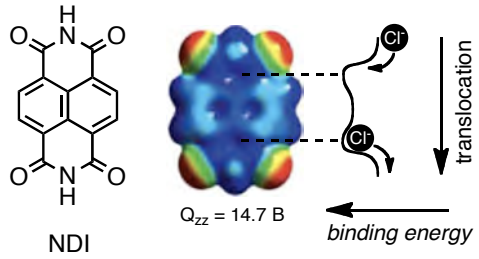

Figure 7. The concept of anion-π transport.

• As fluorescent probes, HPTS (pH sensitive) and CF were used.

• Selectivity sequence for anion transport were determined with HPTS assay (Figure 9, 10, Table 3).

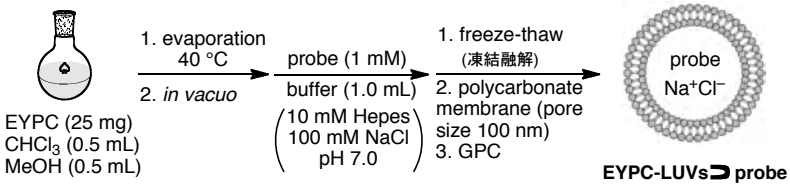

Figure 8. Preparation of prove-containing vesicle.

• EYPC-LUVs ⊃ HPTS were added to buffer (100 mM MCl (M^+ = Li^+, Na^+, K^+, Rb^+, Cs^+) or 100 mM NaX (X^- = F^-, OAc^-, Cl^-, NO_3^-, Br^-, I^-, SCN^-, ClO_4^-, SO_4^{2-}), pH 7.0). Time-dependent change in fluorescene intensity was monitored (Figure 9, 10).

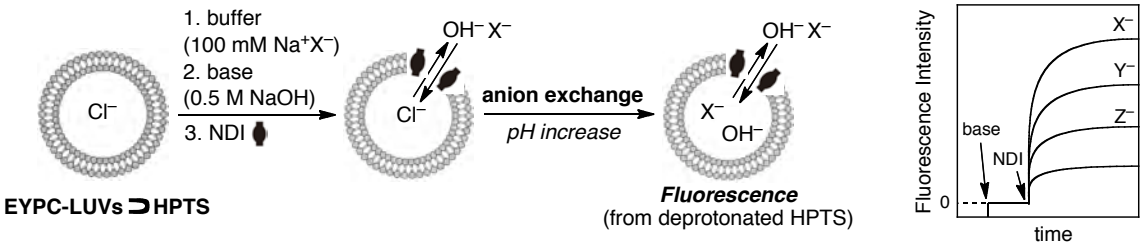

Figure 9. The HPTS assay for anion antiporter.

transport activity: $X^- > Y^- > Z^-$

Table 3. Summary of transmembrane transport data for NDI **2-11**.

Entry	NDI	Cl^-/I^-	Cl^-/Br^-	NO_3^-/AcO^-	Na^+/K^+	EC_{50} (μM)	
						HPTS	CF
1	**3**	–	1.0	–	1.0	150 ± 20	> 100
2	**4**	**2.2**	1.1	0.7	1.0	27 ± 1	17 ± 2
3	**5**	**2.4**	**1.1**	0.8	1.0	37 ± 2	10 ± 1
4	**6**	2.1	**1.5**	**6.0**	1.0	**0.33 ± 0.03**	> 100
5	**2**	1.8	1.4	2.8	1.0	22 ± 2	95 ± 8
6	**8**	–	1.2	0.7	1.0	110 ± 20	–
7	**9**	1.6	1.0	0.8	1.0	32 ± 1	8.0 ± 0.7
8	**10**	**9.0**	1.3	0.4	1.3	7.8 ± 0.7	4.5 ± 0.1
9	**11**	**1.1**	**1.1**	**1.0**	1.0	8.7 ± 1.4	8.2 ± 0.2

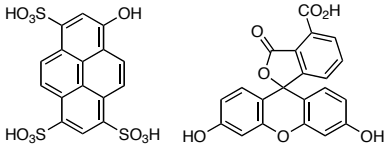

EC_{50} is the effective monomer concentration needed to reach 50% activity.
e.g. EC_{50} (HPTS) < EC_{50} (CF) demonstrates that ion transport is more efficient than dye export or vesicle destruction.

Single-leaflet bundles (NDI 3–6, 9)

• NDI **3** was inactive; decrowded and π-acidified NDI **4** and **5** were clearly more active (Entry 1–3)

➢ Decrowding and π-acidification improve the activity.

• The anion selectivity sequence of NDI **4** and **5** showed increasing activity with increasing hydration energy (Entry 1–3, Figure 10a, 10b).

➢ Strong binding to the transporter to overcompensate the cost of at least partial dehydration.

➢ π-acidity and active-site decrowding govern halide selectivity ($Cl^- > Br^- > I^-$).

• Decrowded and π-acidified NDI **6** exhibited nanomolar activity in HPTS, whereas CF assay was not detectable (Entry 4, Figure 10c).

Vertical crosslinking (NDI 2)

• Stabilization of the active dimeric bundles by vertical crosslinking resulted in an intermediate selectivity (Entry 5, Figure 10d).

Horizontal crosslinking (NDI 8)

• Formal horizontal crosslinking resulted in loss in activity (Entry 6)

➢ NDIs don not act as anion carriers.

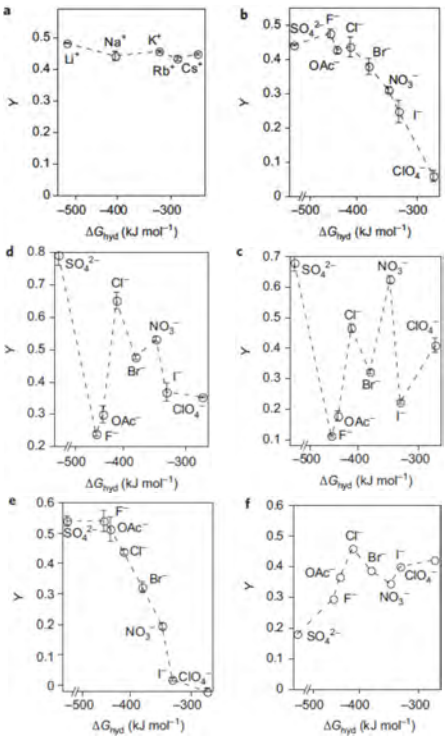

Figure 10. Transport selectivity. Dependence of the fractional transport activity *Y* of NDIs **4** (**a**, **b**), **6** (**c**), **2** (**d**), **10** (**e**) and **11** (**f**) in the HPTS assay.

Hydrophilic anchoring (NDI 10, 11)

• Negatively charged NDI **10** gave outstanding halide selectivity without oxyanion recognition or CF exclusion (Entry 10, Figure 10e).

➢ Charge repulsion at the termini position would loosen the active suprastructure, minimizing the π, π-enhanced anion-π interactions accounting for nitrate selectivity (because nitrate is planar oxyanion with many π-bonds, π-π interaction in π-anion-π complex can be possible.) but provide free access to anion-π bindin sites on monomer surfaces, accounting for chloride selectivity.

• Positively charged NDI **11** delete all meaningful selectivity (Entry 11, Figure 10f).

3. Conclusion

• Direct evidence for the anion-π interactions is obtained by tandem mass spectrometric experiments with NDI models where only the π-acidic surface is left for anions to interact with.

• π-acidity and active-site decrowding are found to govern halide selectivity ($Cl^- > Br^- > I^-$).

• Supramolecular organization accounts for oxyanion selectivity ($NO_3^- > ClO_4^- > SO_4^- > AcO^-$).

4. References

1. Schottel, B. L.; Chifotides, H. T.; Dunbar, K. R. *Chem. Soc. Rev.* **2008**, *37*, 68–83.
2. Gamez, P.; Mooibroek, T. J.; Teat, S. J.; Reedijk, J. *Acc. Chem. Res.* **2007**, *40*, 435–444.
3. Gokel, G. W.; Bollot, G.; Mareda, J.; Matile, S. *Org. Biomol. Chem.* **2007**, *5*, 3000–3012.
4. Mareda, J.; Matile, S. *Chem. Eur. J.* **2009**, *15*, 28–37.